Calibration algorithms of RPC detectors at Daya Bay Neutrino Experiment

2013 JINST 8 T03007

(http://iopscience.iop.org/1748-0221/8/03/T03007)

PUBLISHED BY IOP PUBLISHING FOR SISSA MEDIALAB

RECEIVED: *January 11, 2013*
ACCEPTED: *February 14, 2013*
PUBLISHED: *March 18, 2013*

TECHNICAL REPORT

Calibration algorithms of RPC detectors at Daya Bay Neutrino Experiment

Z. Ning,[a,c,d] **Q.M. Zhang,**[b,1,2] **J.L. Xu,**[d] **L. Lebanowski,**[e] **J.W. Zhang,**[a,d] **C.G. Yang,**[d] **M. He,**[d] **J. Zhao,**[a,c,d] **J.H. Zou,**[d] **V. Pěč,**[f] **Sh.-K. Lin,**[e] **M.Y. Guan,**[d] **H.F. Hao,**[a,g] **L. Zheng,**[a,g] **X.L. Ji,**[a,d] **F. Li,**[a,d] **K. Lau**[e] **and V. Vorobel**[f]

[a] *State Key Laboratory of Particle Detection and Electronics, Beijing 100049, China*
[b] *Xi'an Jiaotong University, Xi'an 710049, China*
[c] *University of Chinese Academy of Sciences, Beijing 100049, China*
[d] *Institute of High Energy Physics, Chinese Academy of Sciences, Beijing 100049, China*
[e] *Department of Physics, University of Houston, Houston, TX 77204-5005, U.S.A.*
[f] *Faculty of Mathematics and Physics, Charles University, Prague 12116, Czech Republic*
[g] *University of Science and Technology of China, Hefei 230026, China*

E-mail: zhangqingmin@mail.xjtu.edu.cn

ABSTRACT: During the commissioning of RPC detector systems at the Daya Bay Reactor Neutrino Experiment, calibration algorithms were developed and tuned, in order to evaluate and optimize the performance of the RPC detectors. Based on a description of the hardware structure of the RPC detector systems, this paper introduces the algorithms used for detector calibration, including trigger rate, efficiency, noise rate, purity and muon flux.

KEYWORDS: Analysis and statistical methods; Data processing methods; Simulation methods and programs

[1] Corresponding author.
[2] Was affiliated with Institute of High Energy Physics, Chinese Academy of Sciences, Beijing 100049, China.

doi:10.1088/1748-0221/8/03/T03007

Contents

2013 JINST 8 T03007

1 Introduction

The Daya Bay Reactor Neutrino Experiment [1] aims at the precise measurement of the neutrino mixing angle θ_{13} by comparing observed Inverse Beta Decay (IBD) event rates at both near and far baselines from six nuclear reactors. At Daya Bay, there are three Experiment Halls (EHs): two halls (EH1 and EH2) nearer to the reactors and one hall (EH3) farther from the reactors. The most recent result from the Daya Bay experiment is $\sin^2 2\theta_{13} = 0.089 \pm 0.010$ (stat.) $\pm$ 0.005 (syst.) [2, 3]. The majority of the systematic uncertainty is due to backgrounds induced by cosmic-ray muons. To minimize these uncertainties, the Antineutrino Detectors (ADs) [4] are deployed underground with redundant muon veto systems. A muon veto system consists of a water Cherenkov pool and an RPC (Resistive Plate Chamber) detector array. As shown in figure 1, the ADs are immersed in the water pool, which tracks muons and shields from ambient radioactivity. The RPCs are located above the water pool and independently detect muons.

The RPC has been widely applied in high energy physics experiments such as BaBar [5], Belle [6], ALICE [7], ATLAS [8], CMS [9, 10], ARGO-YBJ [11] since its invention in the 1980s [12]. It continues to be studied as a candidate active medium for a digital hadron calorimeter [13–17]. Bakelite RPCs, developed by Institute of High Energy Physics (IHEP), Chinese Academy of Sciences (CAS), have been successfully applied to BESIII as a muon identifier [18–22], and were further developed for neutron detection [23] and a digital hadron calorimeter [24] later on. Based on the experience from BESIII and studies implemented to meet

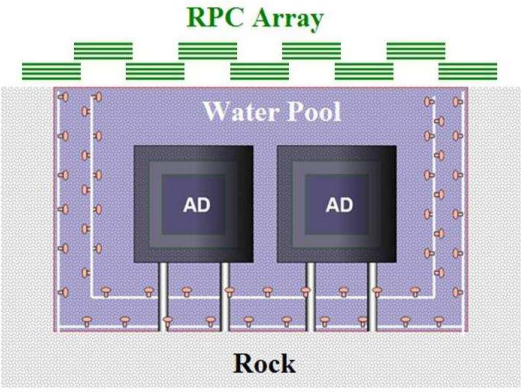

Figure 1. Layout of sub-detectors at one site.

the specific requirements of Daya Bay, RPC technology was adopted to construct an underground cosmic-ray detector [25–30].

2 Components of the RPC detector system

An RPC detector system is composed of RPC modules, a gas system, a high voltage (HV) system and an electronic readout system. In addition, a Detector Control System (DCS) is used to monitor and control the gas and HV systems as well as monitor environmental temperature, pressure and humidity.

2.1 RPC modules

The RPC arrays in both EH1 and EH2 consist of 6 × 9 modules (9 × 9 modules in EH3). The RPC modules are deployed on a movable support structure as seen in figure 2. During commissioning, an RPC array stayed in an 'RPC hall' to the side of the pool, while it was moved into the designed position along the RPC support railway for normal data taking. At each site, two supplementary "telescope" RPC modules are installed at two opposing banks of the water pool, approximately 2 m above the top of the RPC array (see figure 2).

Figure 3 shows the relative positions of RPC modules on a support structure. The 10 cm overlap on all sides among adjacent modules aims to minimize dead regions [29]. Module dimensions are 2.17 m × 2.20 m × 0.08 m. The inner structure of modules is shown in figure 4. Each module consists of 4 layers and each layer contains one 'small' RPC (1.00 m × 2.10 m) and one 'big' RPC (1.10 m × 2.10 m), as shown in the top right diagram of figure 4. In addition the placement of the two RPCs varies among layers to reduce overlapping dead regions due to RPC edges (0.024 m × 2.10 m). The RPCs themselves are bakelite RPCs with a single 2.0 mm-thick gas gap, and the total area of RPC is 3200 m^2.

RPC signals are read out from copper-clad sheets of FR-4. Each sheet is divided into four readout strips, 2.1 m × 0.26 m in size and with a zigzag design as shown in the bottom right diagram of figure 4. The performance of this type of readout strip is equivalent to one with dimensions of 8.4 m × 6.5 cm. This zigzag design changes the impedance to give a higher and narrower pulse,

2013 JINST 8 T03007

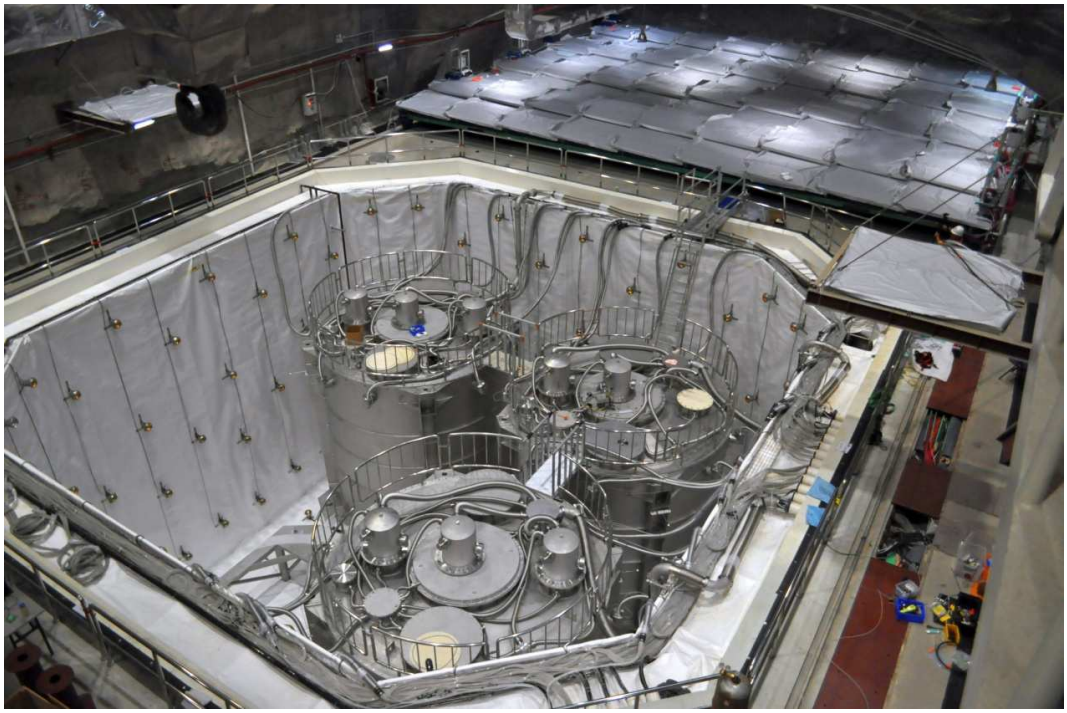

Figure 2. EH3: RPC array in the RPC hall. It moves to/away from the top of the water pool by motor and railway.

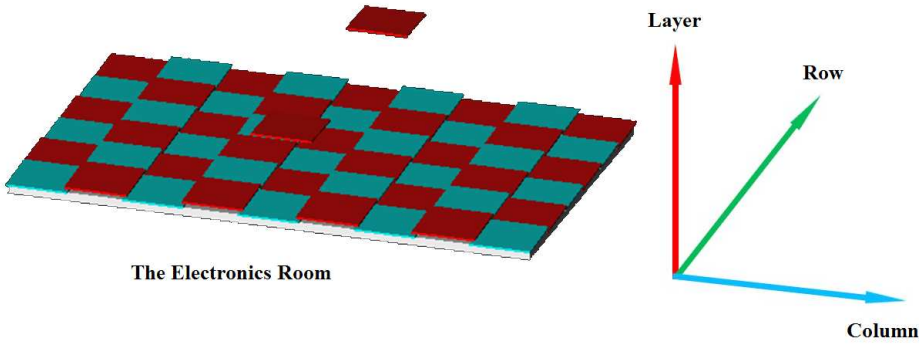

Figure 3. Layout of RPC modules.

which would otherwise require more readout channels [27]. One end of each strip is connected to the input of a Front-End Circuit (FEC), while both ends are connected to a clean ground through a 27 Ω resistor determined by a test. Each layer of RPCs is covered by two readout sheets together, giving each module a total of 32 readout strips (4 strips/sheet × 2 sheets/layer × 4 layers). As illustrated in figure 4, strips on the 1st and 4th layers (counting from the bottom) are in the 'X' direction, and the strips on the 2nd and 3rd layers are in the 'Y' direction, which is parallel to the RPC support railway.

2013 JINST 8 T03007

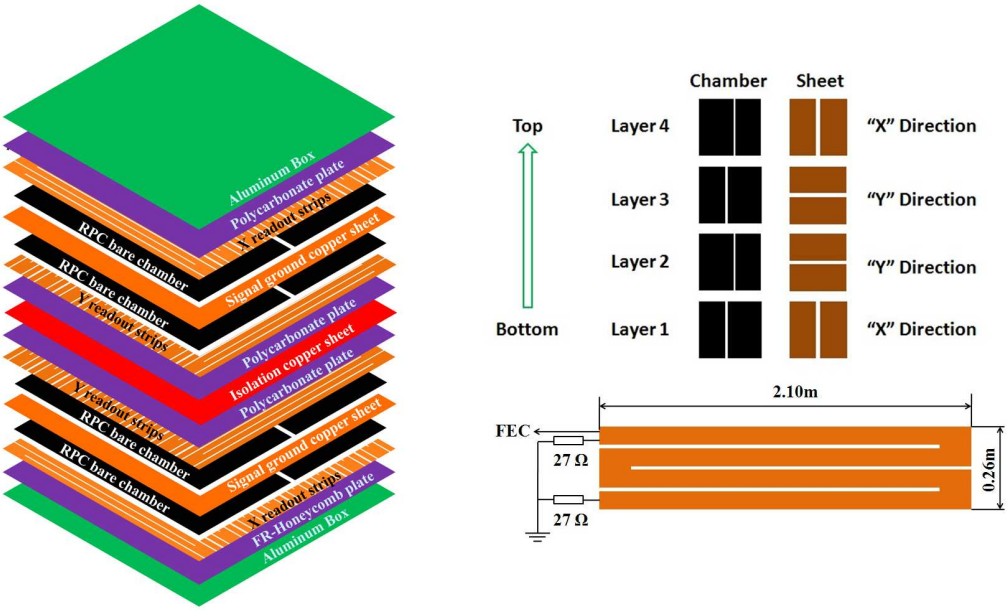

Figure 4. The inner structure of an RPC module.

2.2 Gas and HV systems

At each site, a gas system consists of gas cylinders, a gas mixing and fire detector safety monitoring system, a gas distribution system and a gas chromatograph. The RPCs operate in streamer mode with a gas mixture of Ar: $C_2H_2F_4$: i-C_4H_{10}: SF_6 = 65.5: 30: 4: 0.5 [28], which is controlled by a mass flow control system (MKS 247D). The flow rate at each site is about 1 RPC-volume per day.

The HV system consists of mainframes, fan-out boxes and HV interface boxes. The RPC HV is optimized at 7600 V. The entire HV system is monitored and controlled remotely by a DCS. Moreover, the HV and gas systems are interlocked through the DCS for the safety of the RPCs. In the case of an alarm signal from the gas system, the HV DCS will warn the personnel in the control room and allow them 30 minutes to resolve the issue before automatically turning off the RPC HV.

2.3 Readout electronics system

In each hall, the electronics system consists of FECs, ReadOut Transceivers (ROTs), a VME crate and two VME modules: an RPC Trigger Module (RTM) and a ReadOut Module (ROM) [31]. A detailed diagram is shown in figure 5. The signals from all 32 strips in a single RPC module are read out by a single FEC. The hit information (1 or 0) for every strip is obtained by discriminating the signal with the internal discriminators of the FECs. If three or all four layers within one RPC module have hits simultaneously, a local trigger will be generated by the FEC (a '3/4' trigger), and then sent to the RTM through an ROT. At the same time, the FEC data is temporarily stored in a shift register. Upon the arrival at the FEC of a readout trigger from the RTM, the FEC data is transferred to an event buffer. In order to match the RTM readout trigger with its corresponding FEC data within a signal window (T_w = 25 ns/clock cycle $\times$ 16 clock cycles = 400 ns), an adjustable trigger

2013 JINST 8 T03007

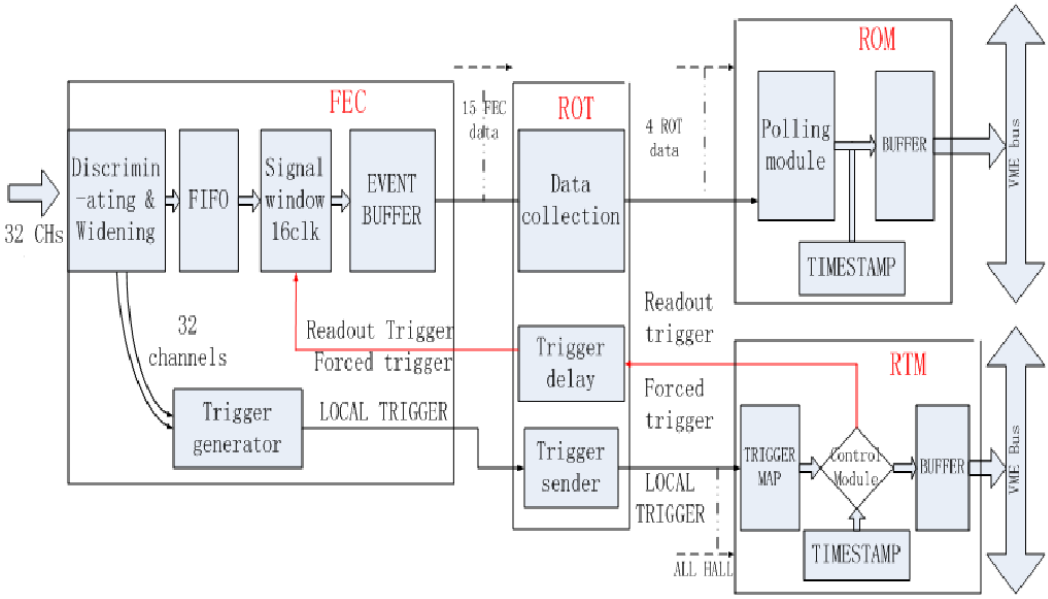

Figure 5. The architecture of the RPC electronics system.

latency time is introduced. A proper latency setting has been determined onsite through trigger rate testing (see section 3.2.1) and is configurable through the Data Acquisition (DAQ) system. The resulting data are buffered in the ROM before being transmitted to the DAQ system by VME bus. The data packages are read out by the means of polling and sorting online according to time stamps [32]. The locally generated 3/4 triggers read out a single RPC module only. Additionally, in order to measure RPC noise rate, a periodic forced trigger reads out all hit information from all FECs at 10 Hz during normal data taking.

3 Calibration algorithms

The calibration algorithms were developed and tuned in order to evaluate and optimize the performance of the RPC detectors. Based on the previous description of the hardware structure of the RPC detector systems, this section introduces the algorithms for detector calibration including trigger rate, efficiency, noise rate, purity and muon flux. The algorithms are tuned by using experimental data and theoretical models, and implemented within RPC software. The RPC software includes both online and offline components. The former is used to monitor detector performance during data taking and the latter is used for detector calibration and physics analysis. Here, only the calibration algorithms of the offline software are discussed.

3.1 Offline software

RPC offline software includes simulation [26], detector calibration and event reconstruction [30], and runs in the Daya Bay offline software framework, called NuWa, which is developed based on Gaudi [33]. Muon simulation data is generated using Geant4 according to the surveyed mountain geometry. Experimental data, including event time, trigger type (3/4 or 2/4 trigger type, the

2013 JINST 8 T03007

latter being from the original design and unused) and lists of hits with coordinates, are used to reconstruct physics events. Physics events are analyzed based on the LAF (Lightweight Analysis Framework) [34] and used to calibrate detector performance and reconstruct muon information (incident positions or/and tracks). Simulation results and calibration algorithms are validated and tuned by comparison with experimental data.

3.2 Detector calibration

The offline calibration of RPC performance includes determination of the efficiency and noise rate of each layer in an RPC module. The calibration algorithms were developed to account for the structure of an RPC module, the layout of RPC modules, the readout mechanism and the anchoring position of an RPC array, and will be described in the following sections.

3.2.1 Trigger rate

As mentioned above, RPC data is sorted online by the DAQ system and then packed following these criteria: RTM triggers within a time window of three clock cycles (75 ns) are treated as belonging to the same event, and a matching is performed between an RTM trigger and FEC data if their time difference is within one clock cycle. Under these criteria of online sorting, the 3/4 trigger rate of a module is calculated precisely as follows:

$$R_{3/4} = \frac{N_{3/4}}{A \times \Delta T},$$

where $N_{3/4}$ is the number of events which have 3 layers or all 4 layers with hits, A is the effective area of a layer ($2.08\,\mathrm{m} \times 2.06\,\mathrm{m} = 4.28\,\mathrm{m}^2$), and ΔT is the time length of data-taking. Similarly, the 4/4 trigger rate of a module is also calculated precisely as follows:

$$R_{4/4} = \frac{N_{4/4}}{A \times \Delta T},$$

where $N_{4/4}$ is the number of events which have all 4 layers with hits.

The 3/4 trigger rates in EH1, EH2, and EH3 are 200, 130, and 40 Hz, respectively. Figure 6 shows the dependence of the 3/4 trigger readout rate on trigger latency in EH1. According to the setting of the electronics, the width of the plateau should be the width of signal window (T_w is 16 clock cycles), which is consistent with the observation in figure 6. It is clearly seen that data loss occurs when the latency is out of the range (45, 60) clock cycles. Accordingly, a latency value of 54 clock cycles was chosen, which is almost in the middle of the usable range.

3.2.2 Efficiency

3.2.2.1. Layer efficiency

Since the RPC detector is used as an anti-coincidence detector for muons at Daya Bay, it is critical to determine the muon detection efficiency precisely. The RPC layer efficiency is calculated as follows:

$$\varepsilon_i = \frac{N_{ijkl,R1,R2}}{N_{jkl,R1,R2}},$$

where $i,j,k,l \in \{1,2,3,4\}$ and none of i,j,k and l are equal, ε_i is the efficiency of layer i in a given module, $N_{ijkl,R1,R2}$ is the number of 4-fold coincidences involving all 4 layers and $N_{jkl,R1,R2}$

2013 JINST 8 T03007

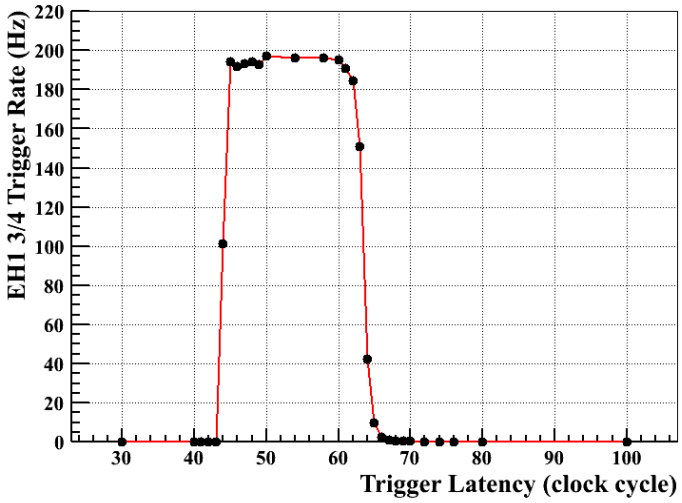

Figure 6. The trigger rate versus trigger latency in EH1.

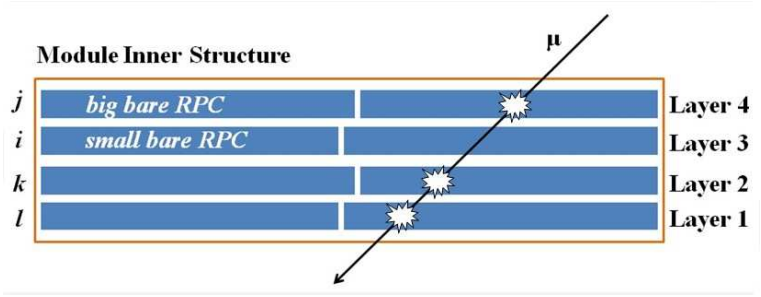

Figure 7. Example of a 3-fold event used in the calculation of the efficiency of layer *i*.

is the number of 3-fold coincidences of layers j, k and l. The meanings of R1 and R2 are explained below. Figure 7 (not to scale) illustrates one example of a $N_{jkl,R1,R2}$ event.

In order to select muons with high purity, two requirements are introduced. The first requirement (R1), which aims to suppress cross-talk, is that no more than two strips are fired in each layer of the triggered modules (the two fired strips should be adjacent). The second requirement (R2) is that the Water Cherenkov Pools tag a muon within 600 ns of an RPC 3/4 trigger. R2 reduces the effect of underestimating the efficiency due to accidentals and all other purely RPC-related backgrounds, which are more significant in underground measurements than at sea level. Before R2 is applied, the calculated average efficiencies of three randomly selected layers in three randomly selected modules from EH1, EH2 and EH3 are (96.42 $\pm$ 0.03)%, (95.9 $\pm$ 0.03)% and (80.77 $\pm$ 0.25)%, respectively. However, when R2 is applied, the corresponding efficiencies are (97.04 $\pm$ 0.03)%, (96.88 $\pm$ 0.03)% and (97.06 $\pm$ 0.13)%, which are consistent with the test results at sea level in IHEP, Beijing [29]. The larger difference of 17% in EH3 is due to the lower muon flux (muon flux is discussed in section 3.2.5). Figure 8 shows the effect of R2 in EH3 for each layer of RPCs.

Given that R2 makes use of the water pool, there is a concern that a muon angle selection bias may cause a bias in calculated efficiency. Due to the limited spatial resolution and selection

2013 JINST 8 T03007

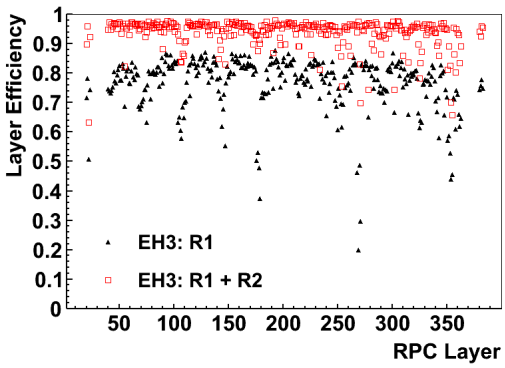

Figure 8. Comparison of calculated layer efficiencies with and without R2.

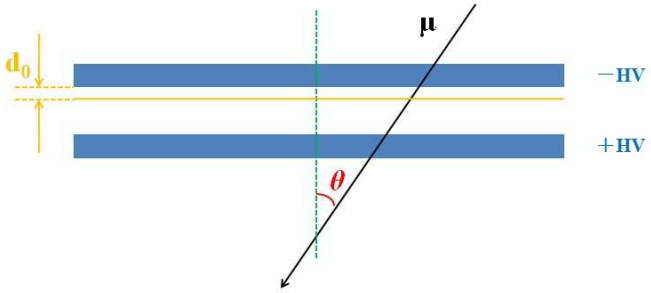

Figure 9. Estimation of efficiency bias due to angle selection of muons.

bias of muon tracks supplied by all detectors, the angle selection bias of R2 must be investigated theoretically. Daya Bay RPCs work in streamer mode; therefore, theoretically only primary ionizations generated within a distance d_0 from the inner surface of the cathode plate can produce a detectable streamer signal as shown in figure 9. Accordingly, the dependence of efficiency (ε) on muon incident angle (θ) can be written as

$$\varepsilon(\theta) = 1 - P(X = 0|\theta) = 1 - e^{-\frac{nd_0}{\cos\theta}},$$

where P(X=0|θ) denotes the Poisson probability that there are no primary ionizations within the distance d_0, and n is the average number of ionizations per unit track length.

If the efficiency for vertical muons (θ = 0) is known, the formula takes the form

$$\varepsilon(\theta) = 1 - e^{\frac{\ln(1-\varepsilon(0))}{\cos\theta}}.$$

Assuming $\varepsilon(0)$ = 95%, we can get the dependence of efficiency on incident angle θ. For each experimental hall, the angular distribution of muons is known from simulation. The bias is estimated by simulation with the detector's survey geometry and the angular distribution. As figure 10 shows for EH3, the simulation predicts a bias that ranges from about - 0.55% to + 0.55% with an average of - 0.07%. Ultimately, any discrepancy in the estimated bias will be small and worth the improvement in calculated efficiency (2% for EH1 and EH2 and 17% for EH3).

2013 JINST 8 T03007

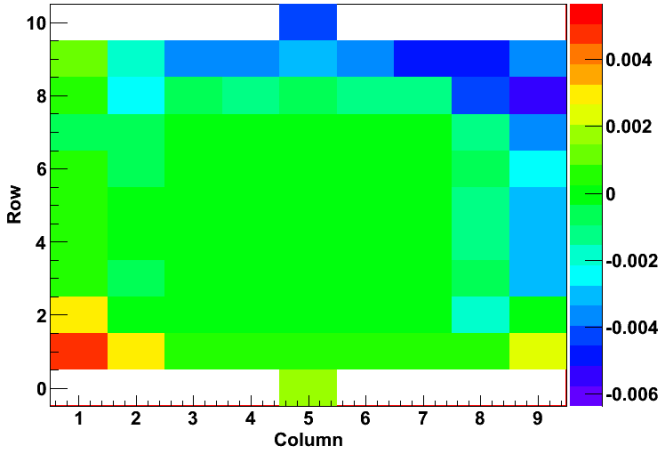

Figure 10. Estimation of efficiency bias due to the angle selection bias of R2 when $\varepsilon(0) = 95\%$ in EH3.

The aforementioned algorithm for calibrating layer efficiency is not directly validated by an independent measurement. We have validated it implicitly by comparing a computation of overall RPC array efficiency using the calibrated layer efficiencies with a measurement of overall RPC array efficiency. The overall efficiency of the RPC module array cannot be determined analytically due to the overlap among RPC layers and RPC modules, gaps between RPC modules and the spatial relationships between the RPC detectors, water Cherenkov pools and Antineutrino detectors. Therefore, it is estimated by simulating the real detector geometry with the calibrated layer efficiencies. This result is compared with a measurement made by selecting muons that pass through the inner half (closer to the RPC array) of either of the two telescope RPC modules and a water pool, which ensures that these muons pass through the RPC array. The computed and measured efficiencies in EH3 are 95.3% $\pm$ 0.6% and 95.8% $\pm$ 0.7%, respectively, which are in agreement.

3.2.2.2. Module efficiency

Given that a trigger must have three or more layers with hits, the 3/4 efficiency of a module, $\varepsilon_{3/4}$, is calculated as follows:

$$\varepsilon_{3/4} = \prod_{i=1}^{4} \varepsilon_i + \sum_{i=1}^{4} \left((1-\varepsilon_i) \prod_{\substack{j=1 \\ j\neq i}}^{4} \varepsilon_j \right).$$

The 4/4 efficiency, $\varepsilon_{4/4}$, is simply the first term in the expression for $\varepsilon_{3/4}$, i.e.,

$$\varepsilon_{4/4} = \prod_{i=1}^{4} \varepsilon_i.$$

Given that the layer efficiencies of a randomly selected module are (95.36 $\pm$ 0.15)%, (97.56 $\pm$ 0.11)%, (95.76 $\pm$ 0.14)% and (97.02 $\pm$ 0.12)% for layers 1, 2, 3 and 4, $\varepsilon_{3/4}$ is (99.28 $\pm$ 0.03)% and $\varepsilon_{4/4}$ is (86.43 $\pm$ 0.24)%.

3.2.3 Noise rate and accidentals

The RPC noise level is indicated by noise rate and dark current. The layer noise rate, which can be used for detector monitoring and the estimation of accidentals and purity (see section 3.2.4), is

2013 JINST 8 T03007

defined as

$$f_i = \frac{N_i}{A \times n \times T},$$

where f_i is the noise rate of layer i in one module, N_i is the number of noise hits in layer i during forced triggers (if a layer has much cross-talk, it is significant to apply R1 in counting N_i), n is the number of forced triggers, and T is the sampling time of each forced trigger (T = width of signal window (T_w) + typical width of digitized RPC signal (T_s) = 400 ns + 150 ns = 550 ns).

Accidental events are one type of event that reduces the purity of RPC triggers. The rate of accidental coincidence of three out of four layers in a module can be estimated using the following formula:

$$R_{3/4,\mathrm{Acc}} = \frac{1}{T_s}\left(4\prod_{i=1}^{4} AT_s f_i + 3\sum_{i=1}^{4}\left((1 - AT_s f_i)\prod_{\substack{j=1 \\ j\neq i}}^{4} AT_s f_j\right)\right),$$

where the typical width of a digitized RPC signal, T_s, is taken to be 150 ns.

The rate of accidental coincidence of four out of four layers is estimated as follows:

$$R_{4/4,\mathrm{Acc}} = 4A^4 T_s^3 \prod_{i=1}^{4} f_i.$$

Given that the layer noise rates of the same module as in section 3.2.2.2 are 586.9 ± 14.1, 537.2 ± 13.5, 571.6 ± 13.9 and 601.2 ± 14.3 Hz/m^2 for layers 1, 2, 3 and 4, the estimated accidental rates of 3 out of 4 layers and 4 out of 4 layers are 0.0160 ± 0.0006 and (4.9 ± 0.2) × 10^{-7} Hz/module, respectively. If R1 is applied, the responded layer noise rates are 583.5 ± 14.1, 532.8 ± 13.5, 567.5 ± 13.9, 598.4 ± 14.3 Hz/m^2, respectively, which means the impact from R1 is below 1%. As mentioned in section 3.2.2.1, R2 minimizes the effects of accidentals and all other RPC-related backgrounds when calculating layer efficiency and it's worth mentioning estimation indicates the accidental rate decreases to the order of 10^{-8} Hz/module if R2 is applied.

3.2.4 Purity

The purity of RPC module triggers is the fraction of real muon events in the triggers. It is calculated as follows:

$$Purity = \frac{N_{3/4,R2}}{N_{3/4}} \times \frac{N_{4/4}}{N_{4/4,R2}},$$

where $N_{3/4,R2}$ and $N_{4/4,R2}$ are the number of 3/4 and 4/4 events under R2, respectively, and the definitions of $N_{3/4}$ and $N_{4/4}$ can be seen in section 3.2.1. This calculation is based on the assumptions that: 1) $N_{4/4}$ counts only muons (which is reasonable because the 4 out of 4 accidental rate is (4.5 ± 0.2) × 10^{-7} Hz/module); 2) Both $N_{3/4,R2}$ and $N_{4/4,R2}$ count only muons (that are also sampled by the water pool); 3) The ratio of the number of true muons in 3/4 events to $N_{3/4,R2}$ is equal to the ratio of $N_{4/4}$ to $N_{4/4,R2}$. Backgrounds enter the calculation of purity through $N_{3/4}$ in the denominator, because 3 layer coincidences are relatively more sensitive to backgrounds. Consequently, the purity of triggers of a randomly selected module in EH1 is about 97.4%.

2013 JINST 8 T03007

Table 1. Comparison of muon fluxes by simulation and measurement using data in all 3 EHs.

	EH1	EH2	EH3
Simulation (Hz/m^2)	0.88 ± 0.09	0.69 ± 0.07	0.039 ± 0.004
Measured by RPC (Hz/m^2)	0.90 ± 0.06	0.69 ± 0.08	0.046 ± 0.004

3.2.5 Muon flux

To minimize contamination from backgrounds in the calculation of muon flux, only the events in which all 4 layers of a module have hits are chosen. Corrections for efficiency, dead time and 4 out of 4 accidental coincidences from noise are taken into account when calculating the muon flux for each module:

$$F_\mu = \frac{\frac{R_{4/4}}{1-R_{3/4}\times A\times T_w} - R_{4/4,\mathrm{Acc}}}{\varepsilon_{4/4}},$$

where the width of the readout trigger, T_w, is 400 ns.

In fact, 3/4 trigger events produce negligible dead time in one second ($= R_{3/4} \times A \times T_w =$ $\sim$1 Hz/m$^2\times$ 4.28 m$^2\times$ 400 $\times$ 10^{-9} s = $\sim 2 \times 10^{-6}$), and the contribution from 4 out of 4 accidentals is even smaller. However, these two factors may be significant for modules with RPCs that have higher noise rates or hot spots. The muon flux in each near (far) hall is obtained by averaging over all 56 (83) RPC modules.

The muon fluxes in the experimental halls predicted by simulation are compared with measurements in table 1. Good agreement is seen for EH1 and EH2, and over-estimation in measurement is seen for EH3 due to the difficulty of rejecting background events, considering its larger background-to-signal ratio.

4 Summary

The offline calibration algorithms of the RPC detector systems of the Daya Bay Reactor Neutrino Experiment have been developed, including trigger rate, efficiency, noise rate, purity and muon flux. The calculated results are cross-checked by using Monte Carlo simulation and theoretical estimation.

Acknowledgments

Institute of High Energy Physics, Chinese Academy of Sciences is supported by the China National Science Foundation and the Ministry of Science and Technology of the People's Republic of China (2006CB808102). This work is also implemented under Project Y2118M005C supported by the National Natural Science Foundation of China, Project 20120201120061 supported by Specialized Research Fund for the Doctoral Program of Higher Education (New Teachers) and the Scientific Research Support Plan for New Teachers (0103-08142036) at Xi'an Jiaotong University. The University of Houston is supported by the United States Department of Energy. Charles University is supported by projects MSM0021620859 and ME08076 of the Ministry of Education, Youth and Sports of the Czech Republic, and 202/08/0760 of the Czech Science Foundation.

2013 JINST 8 T03007

References

[1] DAYA BAY collaboration, *A Precision Measurement of the Neutrino Mixing Angle θ_{13} using Reactor Antineutrinos at Daya Bay*, (2007) [hep-ex/0701029].

[2] DAYA BAY collaboration, F. An et al., *Observation of electron-antineutrino disappearance at Daya Bay*, *Phys. Rev. Lett.* **108** (2012) 171803 [arXiv:1203.1669] [INSPIRE].

[3] DAYA BAY collaboration, F. An et al., *Improved Measurement of Electron Antineutrino Disappearance at Daya Bay*, *Chinese Phys.* **C 37** (2013) 011001 [arXiv:1210.6327] [INSPIRE].

[4] DAYA BAY collaboration, F. An et al., *A side-by-side comparison of Daya Bay antineutrino detectors*, *Nucl. Instrum. Meth.* **A 685** (2012) 78 [arXiv:1202.6181] [INSPIRE].

[5] D. Piccolo et al., *Performances of RPCs in the BaBar experiment*, *Nucl. Instrum. Meth.* **A 515** (2003) 322 [INSPIRE].

[6] BELLE collaboration, Y. Yusa, *Belle muon identification*, *Nucl. Instrum. Meth.* **A 598** (2009) 183 [INSPIRE].

[7] ALICE collaboration, *Commissioning and first performance of the resistive plate chambers for the ALICE muon arm*, *Nucl. Instrum. Meth.* **A 661** (2012) S45.

[8] ATLAS MUON collaboration, *Performance of the ATLAS resistive plate chambers*, *Nucl. Instrum. Meth.* **A 661** (2012) S6.

[9] G. Roselli et al., *Resistive plate chamber commissioning and performance in CMS*, *Nucl. Instrum. Meth.* **A 602** (2009) 696 [INSPIRE].

[10] F. Thyssen, *Performance of the Resistive Plate Chambers in the CMS experiment*, 2012 *JINST* **7** C01104.

[11] ARGO-YBJ collaboration, P. Bernardini, *ARGO-YBJ experiment in Tibet*, *J. Phys. Conf. Ser.* **120** (2008) 062022 [INSPIRE].

[12] R. Santonico and R. Cardarelli, *Development of resistive plate counters*, *Nucl. Instrum. Meth.* **A 187** (1981) 377.

[13] B. Bilki et al., *Calibration of a digital hadron calorimeter with muons*, 2008 *JINST* **3** P05001.

[14] B. Bilki et al., *Measurement of positron showers with a digital hadron calorimeter*, 2009 *JINST* **4** P04006.

[15] B. Bilki et al., *Measurement of the rate capability of Resistive Plate Chambers*, 2009 *JINST* **4** P06003.

[16] B. Bilki et al., *Hadron showers in a digital hadron calorimeter*, 2009 *JINST* **4** P10008.

[17] I. Laktineh, *Development of a semi-digital hadronic calorimeter using GRPC*, *Nucl. Instrum. Meth.* **A 623** (2010) 231 [INSPIRE].

[18] J.-W. Zhang et al., *A new surface treatment for the prototype RPCs of the BESIII spectrometer*, *Nucl. Instrum. Meth.* **A 540** (2005) 102 [INSPIRE].

[19] J.-F. Han et al., *Cosmic ray test results on resistive plate chamber for the BESIII experiments*, *Nucl. Instrum. Meth.* **A 577** (2007) 552 [INSPIRE].

[20] J. Zhang et al., *The design and mass production on Resistive Plate Chambers for the BESIII experiment*, *Nucl. Instrum. Meth.* **A 580** (2007) 1250 [INSPIRE].

2013 JINST 8 T03007

[21] Y. Xie et al., *First results of the RPC commissioning at BESIII*, *Nucl. Instrum. Meth.* **A 599** (2009) 20 [INSPIRE].

[22] J. Zhang et al., *The BESIII muon identification system*, *Nucl. Instrum. Meth.* **A 614** (2010) 196 [INSPIRE].

[23] S. Qian et al., *Study of the RPC-Gd as thermal neutron detector*, *Chin. Phys.* **C 33** (2009) 769.

[24] Q. Zhang et al., *Bakelite RPCs for digital hadron calorimeter*, *Nucl. Instrum. Meth.* **A 654** (2011) 300 [INSPIRE].

[25] Q. Zhang et al., *An underground cosmic-ray detector made of RPC*, *Nucl. Instrum. Meth.* **A 583** (2007) 278 [*Erratum ibid.* **A 586** (2008) 374] [INSPIRE].

[26] M. Guan et al., *Muon simulation at the Daya Bay site*, http://escholarship.org/uc/item/6jm8g76d.

[27] L. Ma et al., *The mass production and quality control of RPCs for the Daya Bay experiment*, *Nucl. Instrum. Meth.* **A 659** (2011) 154 [INSPIRE].

[28] L. Ma et al., *Study of RPC gas composition using Daya Bay RPCs*, *Chin. Phys.* **C 34** (2010) 1116.

[29] J. Xu et al., *Design and preliminary test results of Daya Bay RPC modules*, *Chin. Phys.* **C 35** (2011) 844.

[30] Q. Zhang et al., *Offline software of RPC detector system in Daya Bay Reactor Neutrino Experiment*, *J. Phys. Conf. Ser.* **396** (2012) 022061 [INSPIRE].

[31] H. Hao et al., *Development of VME system in RPC electronics for Daya Bay Reactor Neutrino Experiment*, *Nucl. Sci. Techniques*, accepted, in press.

[32] F. Li, X.-L. Ji, X.-N. Li and K. Zhu, *DAQ architecture design of Daya Bay reactor neutrino experiment*, *IEEE Trans. Nucl. Sci.* **58** (2011) 1723 [INSPIRE].

[33] http://cern.ch/gaudi/.

[34] http://dayabay.bnl.gov/dox/LafKernel/html/annotated.html.

2013 JINST 8 T03007